

Improved Airbreathing Launch Vehicle Performance with the Use of Rocket Propulsion

H. G. Kauffman,* R. V. Grandhi,† W. L. Hankey,‡ and P. J. Belcher§
Wright State University, Dayton, Ohio 45435

An efficient performance analysis method is developed to evaluate potential airbreathing/rocket propulsion systems for advanced technology single-stage-to-orbit launch vehicles. Evaluated are tradeoffs between airbreathing, rocket, and concurrent airbreathing/rocket propulsion in maximizing payload delivery to orbit for a given ascent flight trajectory. With the analysis method, several modes of airbreathing/rocket propulsion are compared to a baseline "airbreather alone" propulsion system in terms of fuel/propellant required to attain orbital velocity. Concurrent airbreathing/rocket propulsion shows a reduction in fuel/propellant consumption over straight airbreather to rocket propulsion transition. The optimal switch point (staging) is identified for the transition from airbreathing to rocket propulsion.

Nomenclature

C_ϕ	= engine throttle ratio
C_L	= coefficient of lift
D	= drag force, N
FA_{STOIC}	= stoichiometric fuel-air ratio
f_s	= P_s/\dot{W} , fuel specific energy, m/kg
G_C	= controller transfer function
G_V	= vehicle transfer function
g	= gravity constant, 9.807 m/s ²
h	= height above sea level, m
I_{SPA}	= airbreather specific impulse, s
I_{SPR}	= rocket specific impulse, s
K	= gain in guidance law
L	= lift force, N
m	= vehicle mass, kg
P_s	= specific excess power, m/s
q	= dynamic pressure, kPa
R	= radius from Earth's center, m
R_E	= Earth radius, 6,356,766 m
S	= vehicle reference area, m ²
s	= distance down range from launch point, m
T	= thrust, N
V	= flight velocity, m/s
W	= vehicle payload, kg
\dot{W}	= airbreather/rocket fuel combined flow rate, kg/s
\dot{W}_{AB}	= airbreather air flow rate, kg/s
\dot{W}_{AF}	= airbreather fuel flow rate, kg/s
\dot{W}_{RP}	= rocket propellant flow rate, kg/s
α	= angle of attack, radians
β	= factor in exponential altitude density relation
γ	= flight-path angle, rad
Δ	= denotes an increment
τ	= time constant in guidance law, s
ϕ	= fuel-to-air equivalence ratio
ρ	= atmospheric density, kg/m ³

Introduction

THE idea of a single-stage-to-orbit vehicle has long been considered by the aerospace community. Studies of airbreathing propulsion in combination with some form of rocket propulsion have appeared in several research papers. Airbreathing propulsion for the atmospheric ascent portion of an Earth-to-orbit trajectory was first proposed by Goddard¹ in 1932. The rationale for such a proposal comes from the fact that airbreathing engines provide about 8–20 times higher effective specific impulse values than pure rockets at altitudes below 30,000 m. Present-day (multiple-stage) rocket launch vehicles consume nearly 80% of their available propellant mass during climb and acceleration through the atmosphere to an altitude of about 58,000 m and 2300 m/s velocity. For some specific vehicle types, a large proportion of this rocket propellant mass can be saved by using a more efficient airbreathing propulsion system until such an altitude is achieved that the rocket begins to attain the greater efficiency. Kramer and Buhler² evaluated this problem for a 1½-stage vertical take-off/landing vehicle and found that airbreathing propulsion is a feasible approach. The concept of a single-stage-to-orbit vehicle using two fuels and rocket propulsion was first proposed by Salkeld³ by operating separate engines in series. Later the dual-fuel engine concept was introduced to reduce the mass of the hydrogen engines.^{4,5} The parallel burn of hydrogen and hydrocarbon engines has been proposed as an alternative to achieve good performance without requiring a dual-fuel engine.^{6–8} Integral rocket/ramjet propulsion has been evaluated, as the theoretical performance of the ramjet propulsion system is much better than either solid- or liquid-fueled rocket motors acting alone.^{9–11} Optimizing the performance of both airbreather and combination airbreather/rocket systems for vehicle delivery to low Earth orbit has been examined with some systems showing considerable promise.^{12–15} Optimizing flight-path trajectories, reducing vehicle size, minimizing fuel expended, etc., all have an effect on the vehicle operating costs, payload delivery to orbit, and mission flexibility.

This paper considers optimizing airbreathing/rocket propulsion for a generic single-stage-to-orbit horizontal takeoff/landing hypersonic vehicle. The primary parameter to be evaluated is when the transition from airbreathing to rocket propulsion should take place. Additionally, the form of transition must be considered, that is, whether switching from airbreather to rocket is most efficient or whether the airbreather engine should be utilized as long as possible by burning the airbreather/rocket engines concurrently.

To screen different conceptual aerospace propulsion systems, the total vehicle system performance must be evaluated. This analysis combines the flight mechanics and aerodynamic

Received May 18, 1990; revision received and accepted for publication Oct. 15, 1990. This paper is declared a work of the U.S. Government and is not subject to copyright protection in the United States.

*Graduate Research Assistant, Department of Mechanical and Materials Engineering. Member AIAA.

†Associate Professor, Department of Mechanical and Materials Engineering. Member AIAA.

‡Professor, Department of Mechanical and Materials Engineering. Fellow AIAA.

§Research Engineer, Department of Mechanical and Materials Engineering.

characteristics with the propulsion features. A numerical simulation must be accomplished and an optimization performed to achieve a favorable design evaluation. The optimization is performed on a personal computer, using a two-degree-of-freedom trajectory simulation, suitable for rapid design trade-off studies. The methodology integrates the equations of motion and tracks velocity, altitude, range, flight-path angle, and vehicle mass. A robust guidance system has been developed to control the "stick and throttle" settings to achieve an optimum flight path for maximum payload delivery into orbit. Once an optimum flight path is chosen (e.g., via the "Energy Method"; see Venugopal¹⁶ et al.), it is then necessary to evaluate the form of propulsion or combination that will achieve the greatest payload delivery to low Earth orbit.

By choosing a single-stage-to-orbit vehicle to study for this problem, both engine and structure weights will be increased over those required for a vehicle utilizing only one form of propulsion. For this investigation, only the vehicle performance has been optimized. In a total design optimization, the weight component study must be incorporated. In spite of this constraint, significant increases in deliverable payload may be accomplished with proper use of airbreather/rocket propulsion.

Trajectory Analysis

The governing equations for planar motion of a point mass are given below. All the quantities in the following equations are given as a function of time:

$$mV\dot{\gamma} = L - mg \cos \gamma + T \sin \alpha + \frac{mV^2}{R} \cos \gamma \quad (1)$$

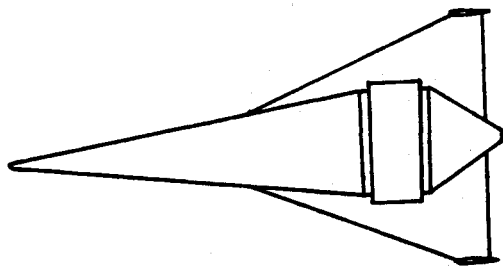


Fig. 1 Study vehicle.

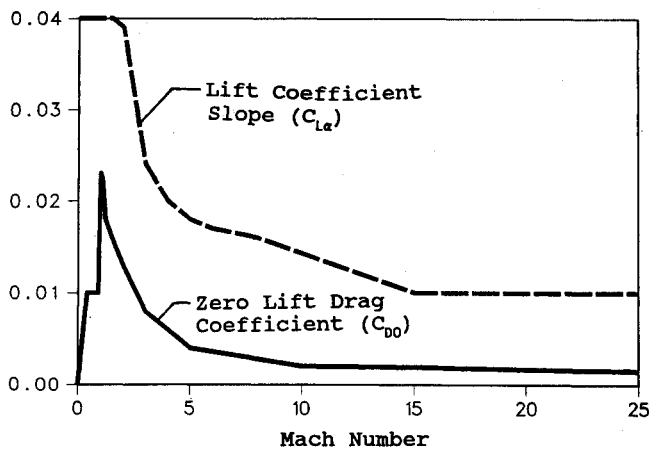


Fig. 2 Vehicle drag and lift characteristics.

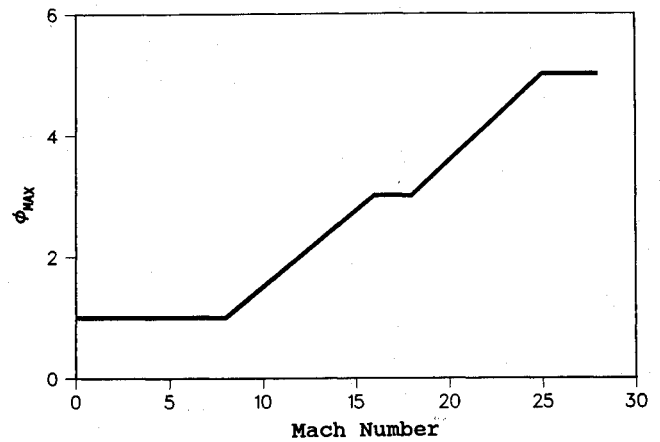


Fig. 3 Maximum equivalence ratio, ϕ_{MAX} .

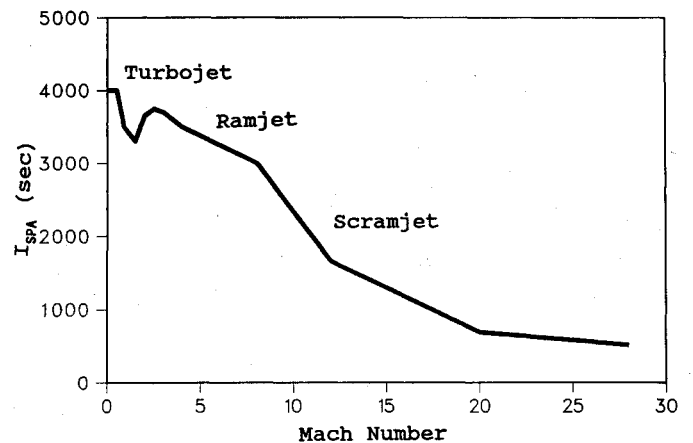


Fig. 4 Airbreather specific impulse, I_{SPA} .

$$m\dot{V} = -D - mg \sin \gamma + T \cos \alpha \quad (2)$$

In addition, the navigation equations required to locate the position of the point mass are

$$\dot{h} = V \sin \gamma \quad (3)$$

$$\dot{s} = V \cos \gamma \frac{R_E}{R_E + h} \quad (4)$$

To control the vehicle, one must command both the "stick" (pitch attitude) and "throttle" (thrust, T) to achieve a desired flight path. For the purposes of this investigation, the guidance law controls the angle of attack α by a second-order rate controller and controls the thrust by limiting the fuel flow (\dot{W}_{AF}) and equivalence ratio ϕ :

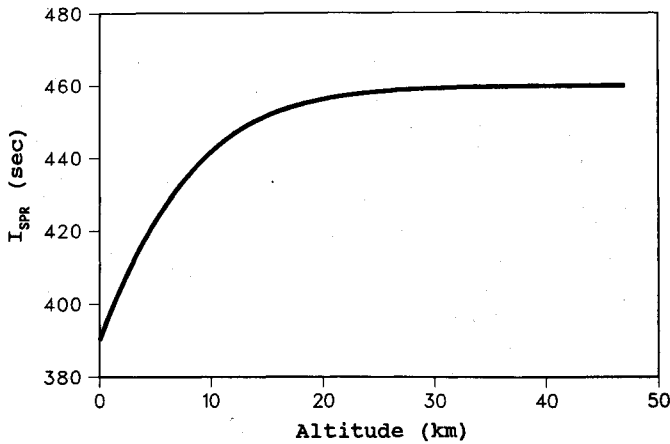
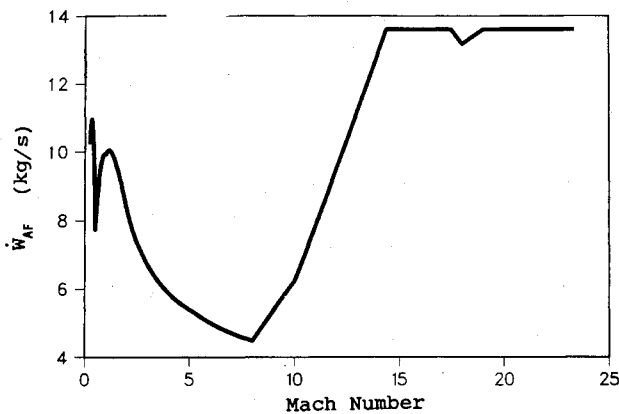
$$T_{AB} = I_{SPA} F A_{STOIC} \phi_{MAX} \dot{W}_{ABMAX} C_\phi \quad (5)$$

where

$$0 \leq C_\phi \leq 1 \quad (6)$$

The governing equations of motion described above are first-order nonlinear ordinary differential equations. To solve these equations, an accurate numerical integration method compatible with the guidance law and optimization procedure is necessary.

A second-order Taylor series integration routine with an adaptive time step provides results comparable to the fourth-order Runge-Kutta method. In addition, computational efficiency is improved, which is an important factor for rapid tradeoff performance studies. The Taylor series method re-

Fig. 5 Rocket specific impulse, I_{SPR} .Fig. 6 Airbreather fuel flow, \dot{W}_{AF} .

quires the computation of higher-order derivatives, but these values are evaluated in an analytical form without the need to loop forward in time and reiterate values.

Earth-to-Orbit Vehicle Description

The vehicle chosen for evaluation is a generic-design hypersonic aircraft. A general view of the aircraft is shown in Fig. 1. The vehicle's aerodynamic and propulsion characteristics are represented graphically in Figs. 2-6. (All vehicle data, including propulsion and aerodynamic characteristics, were obtained from the U.S. Air Force. See Ref. 17.) The objective of this data is to represent values associated with hypersonic vehicles in order to develop the performance methodology. As this data does not pertain to an actual aircraft design, no significance should be given to the specific numerical values. The computed performance was based on the following vehicle properties:

$$W_{TAKEOFF} = 45,360 \text{ kg}$$

$$W_{FUEL} = 27,216 \text{ kg}$$

$$S = 174 \text{ m}^2$$

$$FA_{STOIC} = \text{stoichiometric for } H_2/\text{air} = 0.0292$$

$$\alpha_0 = \text{zero lift angle of attack} = 0 \text{ deg}$$

The system being investigated is subject to constraints determined by the laws of mechanics, aerodynamics, and propulsion. In addition, the vehicle must not exceed specific design constraints imposed by limitations of the structure, materials, flight control, etc. This set of constraints is entitled inequality

constraints and may apply only during portions of the flight. Constraints are imposed on the following parameters:

$$\text{Dynamic pressure} \quad q_{LIMIT} = (\rho V^2)/2 = 47.9 \text{ kPa}$$

$$\text{Acceleration} \quad \dot{V}/g = 1.0$$

$$0 < L/mg < 2.0$$

$$\text{Control effectiveness} \quad \dot{\alpha} \leq 0.05 \text{ rad/s}$$

$$\text{Propulsion cycle} \quad T = T_{MAX}$$

$$\dot{W}_{AFMAX} = 13.6 \text{ kg/s}$$

$$\dot{W}_{RPMAX} = 45.4 \text{ kg/s}$$

Guidance and Control Analysis

The initial strategy was to determine what variables must be controlled, with several choices being explored. It was decided to command altitude as a function of the current velocity since the investigator will usually have some insight into the $(h-V)$ flight corridor early in the investigation.

A guidance law must then be developed that will control the angle of attack α and thrust T to follow the desired $(h-V)$ path. Based upon previous investigations, it was decided to set the thrust to the maximum value T_{MAX} , or $C_\phi = 1$ and $\phi = \phi_{MAX}$, to maximize the payload into orbit. The optimization procedure is developed with T_{MAX} initially, and then perturbed from this value to validate this choice. In any case, $\phi_{MAX}(V)$ will be prescribed. This decision places an extra burden on the α controller to follow the desired flight path when high-thrust-to-weight ratios are present. The control is accomplished by means of a feedback control loop as shown in Fig. 7. It was also decided to use a rate controller for α rather than a displacement controller based on flight experience as well as computer simulations. (In present day aircraft the pitch attitude and pitch rate are controlled through angular acceleration about the Y -body axis. Since we are dealing with a two-degree-of-freedom point mass analysis, the relationship between $\dot{\alpha}$ and the vehicle pitch rate is assumed to be unity for $\Delta t_{me} < 1 \text{ s}$.)

The transfer function for the vehicle G_V is developed using linear theory where the trajectory equations are linearized. (Note: These linear equations will be used only to devise a guidance law and not to ascertain the integrated vehicle payload.) Variations in ΔW , W/D , and ΔD will be neglected for this formulation.

The transfer function may then be obtained and expressed as

$$G_V = \frac{\Delta h}{s \Delta \alpha} = \frac{g \left[\frac{L_1}{(mg)_1} \frac{C_{L\alpha}}{C_{L1}} + \frac{T_1}{(mg)_1} \right]}{s \left[s^2 + \frac{\beta g L_1}{(mg)_1} + \frac{2g^2}{V_1^2} \right]} \quad (7)$$

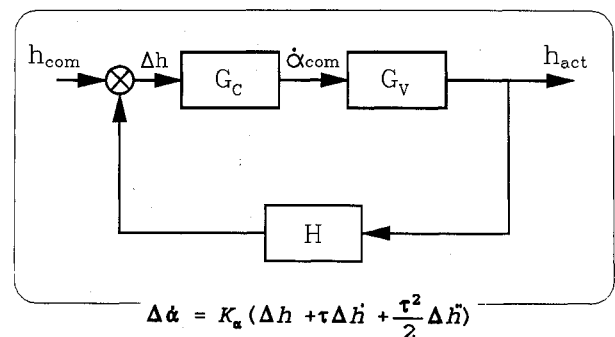


Fig. 7 Vehicle control system.

Over most of the flight path, this transfer function may be approximated as

$$G_V = \frac{qSC_{L\alpha} + T}{ms^3} \quad (8)$$

As stated previously, a second-order rate controller for angle of attack was adopted. It may be expressed as follows:

$$\Delta\dot{\alpha}_{\text{COMMAND}} = K \left(\Delta h + \tau \Delta \dot{h} + \frac{\tau^2}{2} \Delta \ddot{h} \right) \quad (9)$$

where

$$\Delta h = h_{\text{ACTUAL}} - h_{\text{COMMAND}} \quad (10)$$

Expressing the controller transfer function by means of Laplace transforms produces

$$G_C = \frac{s\Delta\alpha}{\Delta h} = K \left(1 + \tau s + \frac{\tau^2 s^2}{2} \right) \quad (11)$$

The goal for the controller is to select the values of the gain K and time constant τ to accurately follow the commanded altitude h_{COMMAND} without burning excess fuel. In addition, the controller must be stable and robust for a variety of flight conditions. Referring back to the feedback loop, the overall transfer function may be expressed as follows:

$$\frac{h_{\text{ACTUAL}}}{h_{\text{COMMAND}}} = \frac{G_C(s)G_V(s)}{1 + H(s)G_C(s)G_V(s)} \quad (12)$$

The characteristic equation for the control system determining the stability features is, therefore,

$$1 + H(s)G_C(s)G_V(s) = 0 \quad (13)$$

let

$$H(s) = -1$$

hence

$$s^3 - \frac{K}{m} (qSC_{L\alpha} + T) \left(1 + \tau s + \frac{\tau^2 s^2}{2} \right) = 0 \quad (14)$$

The gain K was specified as

$$K = \frac{-4m}{\tau^3(qSC_{L\alpha} + T)} \quad (15)$$

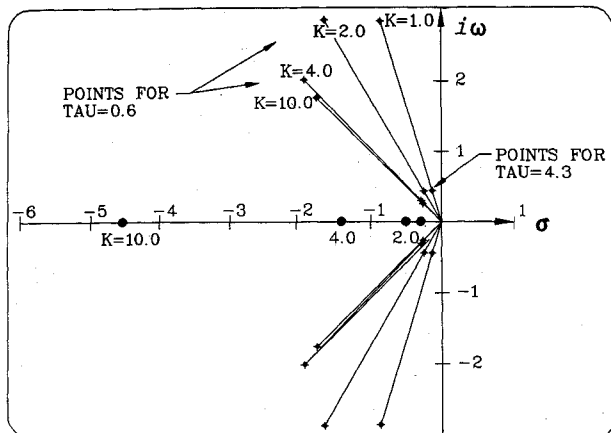


Fig. 8 Control system root locus.

An investigation of the weighing factors for the values of K and τ was then conducted by examining the root locus for the characteristic equation. Figure 8 shows that the control system is stable with all three roots being in the left half-plane. It also shows that increasing K increases damping, and increasing τ increases the characteristic frequency. More importantly, however, Figs. 9 and 10 show that a τ value between 2 and 9 produces the same relative payload values, and a K value between 0.5 and 1.6 produces similar results. For the remainder of the investigation, a τ value of 4.33 and K value of unity (1.0) was utilized. (A time constant of 2.0 and a system gain of 1.4 gave slightly better results for the given case. The increase in payload-to-orbit for these values is insignificant, being measured in hundredths of a percent of the final payload-to-orbit.)

From the guidance law, a set of command equations was developed to meet the vehicle constraints and to follow an altitude vs velocity path [i.e., $h_{\text{COMMAND}}(V)$]. This was accomplished by setting thrust to the maximum value (by prescribing $\phi = \phi_{\text{MAX}}$ and $C_\phi = 1$) and a second-order rate controller on the angle of attack:

$$\Delta\dot{\alpha}_{\text{COMMAND}} = K \left(\Delta h + \tau \Delta \dot{h} + \frac{\tau^2}{2} \Delta \ddot{h} \right) \quad (16)$$

where

$$\Delta h = h_{\text{ACTUAL}} - h_{\text{COMMAND}} \quad (17)$$

$$h_{\text{COMMAND}} = h_{\text{COMMAND}}(V) \quad (18)$$

$$\dot{h}_{\text{COMMAND}} = \left(\frac{\partial h_{\text{COMMAND}}}{\partial V} \right) \dot{V} \quad (19)$$

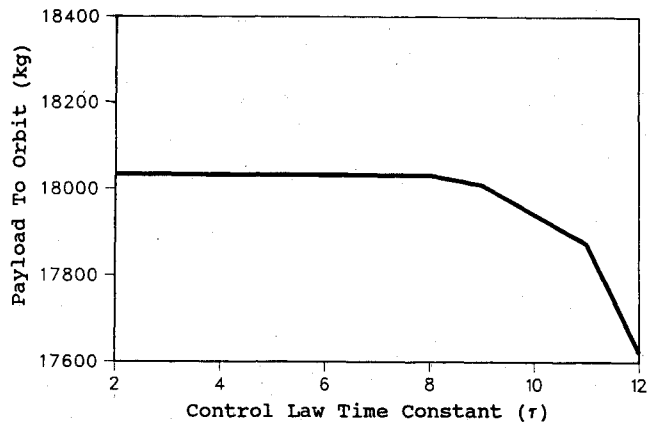


Fig. 9 Payload delivered to orbit vs control law time constant.

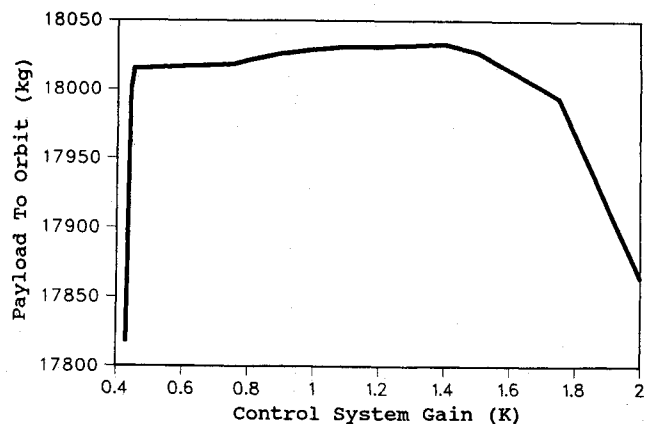


Fig. 10 Payload delivery to orbit vs control law system gain.

$$\dot{h}_{\text{COMMAND}} = \left(\frac{\partial^2 h_{\text{COMMAND}}}{\partial V^2} \right) \dot{V}^2 + \left(\frac{\partial h_{\text{COMMAND}}}{\partial V} \right) \ddot{V} \quad (20)$$

$$\dot{h}_{\text{ACTUAL}} = V \sin \gamma \quad (21)$$

$$\dot{h}_{\text{ACTUAL}} = \dot{V} \sin \gamma + V \dot{\gamma} \cos \gamma \quad (22)$$

Propulsion Systems

The primary objective of this investigation is to maximize the payload delivery into Earth orbit for a single-stage-to-orbit vehicle (i.e., minimize fuel/propellant burned). The question of what rocket size to select may be addressed by using the optimization procedures described below, and by conducting payload delivery-to-orbit vs rocket size trade studies.

The most informative method for gaining insight into the optimum propulsion transition solution is to prepare fuel specific energy ($f_s = P_s / \dot{W}$) contours on an h - V map for the airbreather engine and rocket, both alone and together. Specific excess power P_s may be written as

$$P_s = \frac{d}{dt} \left(h + \frac{V^2}{2g} \right) = \frac{V(T-D)}{mg} \quad (23)$$

The specific excess power is equal to the time rate of change of the specific energy of the vehicle. Plotting the contours of P_s on an h - V map allows the vehicle's flight envelope to be determined for both the airbreathing engine and rocket. These maps for the airbreathing and rocket engines (Figs. 11 and 12) immediately identify the superior areas of performance (h and V) for each propulsion system. The numerical values on the contours indicates the vehicle's specific excess power at that point. This excess power may be traded for gain in altitude or velocity. The most interesting feature that these two maps depict is that the airbreather performance degrades near orbital conditions (i.e., $V = 7860$ m/s); however, the rocket improves. By overlaying the two maps, the regions of superior performance for each system may easily be identified. As seen in Fig. 13, the airbreathing engine maintains superior engine performance up to an altitude of 46,600 m. Above this altitude, the rocket alone shows superior performance.

For the case of maximum payload into orbit, the vehicle should follow the maximum value of f_s between any two energy states. For this case, Fig. 13 indicates that the vehicle should utilize airbreathing propulsion at takeoff, fly to 46,600 m, and then transition to rocket propulsion for ascent to Earth orbit at 185 km. The question then arises: when precisely, should the transition in propulsion take place? It is logical that a single-stage-to-orbit vehicle should utilize its airbreathing engine as long as is practical. This proposes a second question as to whether the operation of both systems separately or simultaneously will produce the goal of maximum payload to orbit.

Optimum Transition Studies

As stated previously, this evaluation will consider a constant dynamic pressure path ($q_{\text{LIMIT}} = 47.9$ kPa). The vehicle will follow an h - V relationship determined by $\Delta \alpha_{\text{COMMAND}}$ and T_{MAX} , where

$$T_{\text{MAX}} = T_{\text{ABMAX}} + T_{\text{ROCKETMAX}} \quad (24)$$

$$T_{\text{ROCKET}} = I_{\text{SPR}} \dot{W}_{\text{RP}} \quad (25)$$

At high altitudes, for a constant q path, the energy gained by a vehicle is primarily a function of velocity. To evaluate the optimum switch point from airbreather to rocket propulsion, it was decided to relate the fuel/propellant flow rate \dot{W} to the rate of change in velocity for the vehicle \dot{V} . This ratio \dot{W}/\dot{V} is plotted against altitude in Fig. 14.

Figure 14 shows three curves of \dot{W}/\dot{V} vs altitude for 1) airbreathing propulsion alone, 2) concurrent airbreathing/

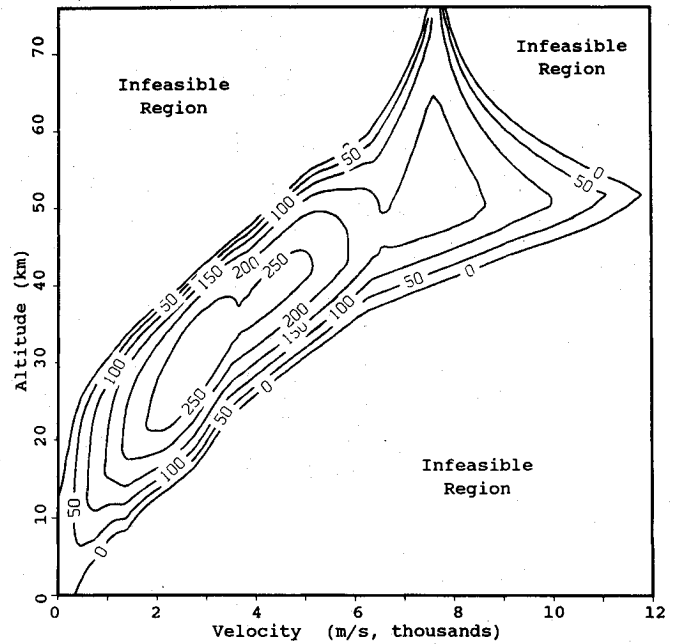


Fig. 11 Airbreather fuel specific energy contours $\times 1.49$ m/kg, $\dot{W}_{\text{AF}} = 13.6$ kg/s.

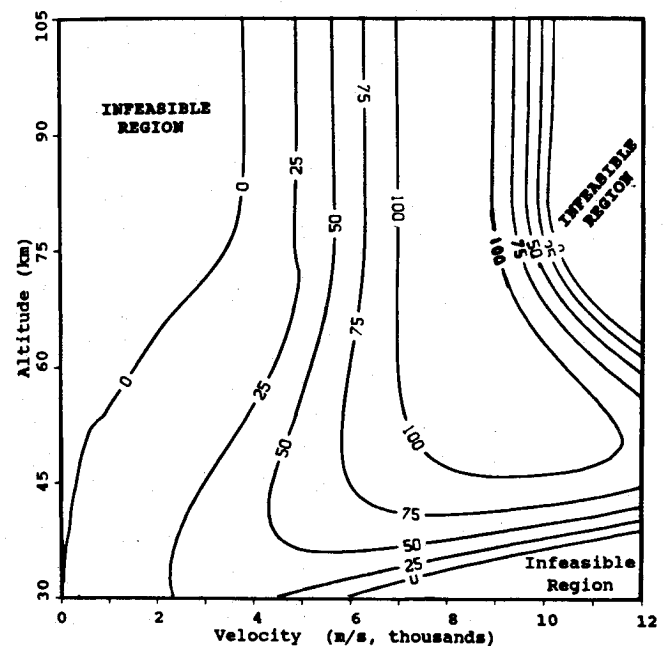


Fig. 12 Rocket fuel specific energy contours $\times 1.49$ m/kg, $\dot{W}_{\text{RP}} = 45.4$ kg/s.

rocket propulsion, and 3) rocket propulsion alone. The area under each curve represents the fuel burned; thus the minimum value of \dot{W}/\dot{V} indicates the best case. Many simulations of the constant dynamic pressure trajectory path to orbital velocity were run for cases where 1) airbreather and rocket utilized for entire mission, 2) airbreather only, 3) transition to concurrent airbreather/rocket, and 4) transition to rocket only. Examining Fig. 14 for the locus of minimum values of \dot{W}/\dot{V} indicates that the airbreather alone burns less fuel for altitudes below 43,900 m. For a 47.9 kPa dynamic pressure (q) path, as the vehicle approaches 43,900 m and a velocity of 6520 m/s the combination of burning both the airbreather and rocket begins to show the greater efficiency. At this point the rocket is turned on and the vehicle accelerates to orbital velocity (approximately 7860 m/s at 46,950 m). Once orbital velocity is

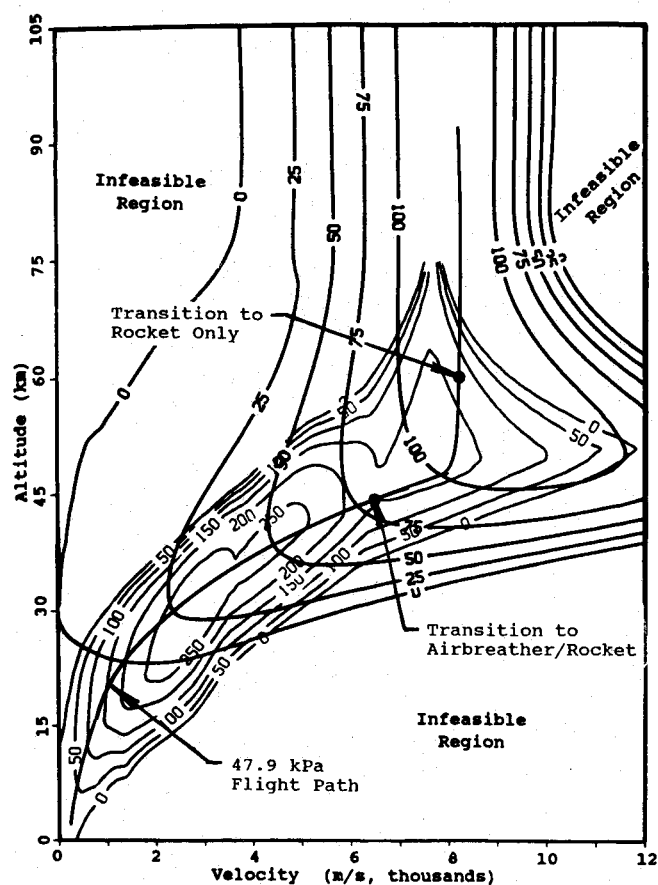


Fig. 13 Comparison of airbreather and rocket fuel specific energy contours $\times 1.49$ m/kg.

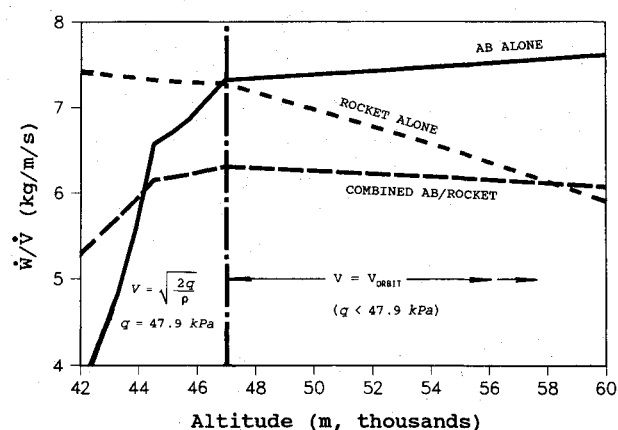


Fig. 14 Comparison of fuel/propellant flow rate relative to change in velocity vs altitude.

reached, the velocity is held constant as the vehicle continues to climb in altitude. Between 43,900 m and 58,850 m, the transition to concurrent airbreather/rocket propulsion burns minimum fuel/propellant. As the vehicle begins to approach 58,850 m, the rocket alone begins to show the greater efficiency and the second propulsion transition should occur. If transition from airbreathing propulsion to rocket were to be made directly, Fig. 14 indicates that this transition should occur at 47,060 m and a velocity of 7830 m/s.

To further substantiate this analysis, several cases were run parametrically using concurrent airbreather/rocket propulsion. For these simulations, the mission is defined as being complete when the vehicle reaches orbital velocity. The final vehicle payload (vehicle mass and excess fuel) for each simulation was plotted against the vehicle velocity at the time the

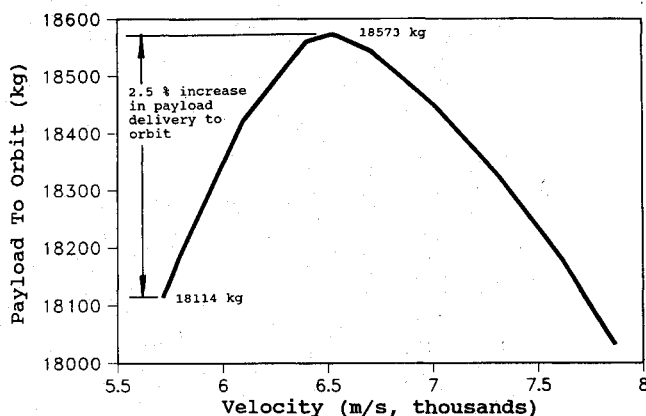


Fig. 15 Optimum rocket turn-on velocity vs final payload at orbital velocity, 47.9 kPa q path.

rocket is turned on. These values of vehicle payload-vs-rocket turn on velocity are plotted in Fig. 15, which confirms that the minimum fuel/propellant burned to achieve orbit occurs with a transition to concurrent airbreather/rocket propulsion at 43,900 m, and results in a final vehicle payload of 18,573 kg. When the mission was run using airbreathing propulsion alone, the final vehicle payload was 18,033 kg. (Fuel required to complete the mission exceeded the fuel available by 111 kg.)

The case where the rocket was burned concurrently with the airbreather from takeoff was clearly inferior, with a final vehicle payload of 10,251 kg. (Fuel required to complete the mission exceeded the fuel available by 7895 kg.)

Conclusions

A methodology has been developed to conduct rapid propulsion trade studies for Earth-to-orbit vehicles. In this paper, a generic design vehicle has been analyzed to demonstrate the procedure. However, some generalized results have evolved. The conclusions from this paper may be summarized, as follows, for the vehicle analyzed:

- 1) Airbreathing propulsion is more efficient than rocket propulsion at lower altitudes.
- 2) Rocket propulsion may be necessary for orbital maneuvering (injection and retrograde) and final climb to the orbital altitude.
- 3) Concurrent airbreathing/rocket propulsion maximizes the use of the airbreather engine for the given vehicle and shows a reduction in fuel/propellant consumption over straight airbreather to rocket propulsion transition.
- 4) Use of a combination airbreather/rocket propulsion system is shown to be more efficient than either an airbreather or a rocket alone for a complete orbital mission.

Acknowledgments

This research was supported by the U.S. Air Force Contract F33615-87-C-1550 through the Center for Artificial Intelligence Applications, Dayton, Ohio.

References

- ¹Goddard, R. H., "A New Kind of Turbine Rocket Plane for the Upper Atmosphere," *Scientific American*, Vol. 146, March 1932, p. 148.
- ²Kramer, P. A., and Buhler, R. D., "Hybrid Rocket/Airbreathing Propulsion for Ballistic Space Transportation," *Journal of Spacecraft and Rockets*, Vol. 17, July-Aug. 1980, pp. 334-341.
- ³Salkeld, R., "Mixed-Mode Propulsion for the Space Shuttle," *Astronautics and Aeronautics*, Vol. 9, Aug. 1971, pp. 52-58.
- ⁴Salkeld, R., and Beichel, R., "Reusable One-Stage-to-Orbit Shuttles: Brightening Prospects," *Astronautics and Aeronautics*, Vol. 11, June 1973, pp. 48-58.
- ⁵Salkeld, R., "Contribution to the Discussion of Mixed-Mode Propulsion and Reusable One-Stage-to-Orbit Vehicles," 23rd International Astronautical Congress, Vienna, Austria, Oct. 8-15, 1972.

⁶Henry, B. Z., and Decker, J. P., "Future Earth Orbit Transportation Systems/Technology Implications," *Astronautics and Aeronautics*, Vol. 14, Sept. 1976, pp. 18-29.

⁷Martin, J. A., "Parallel-Burn Options for Dual-Fuel Single-Stage Orbital Transports," *Journal of Spacecraft and Rockets*, Vol. 15, Jan.-Feb. 1978, pp. 4-6.

⁸Martin, J. A., "A Method for Determining Optimum Phasing of Multi-Phase Propulsion System for a Single Stage Vehicle with Linearized Inert Weight," NASA TN-D7792, Nov. 1974.

⁹Billig, F. S., Waltrup, P. J., and Stockbridge, R. D., "Integral-Rocket Dual-Combustion Ramjets: A New Propulsion Concept," *Journal of Spacecraft and Rockets*, Vol. 17, July-Aug. 1980, pp. 416-424.

¹⁰Readey, H. J., and Cobb, E. R., "Center-Loaded Duct Integral Rocket-to-Ramjet Transition Testing," *Journal of Spacecraft and Rockets*, Vol. 17, March-April 1980, pp. 105-111.

¹¹Webster, F. F., "Integral Rocket/Ramjet Propulsion-Flight Data Correlation and Analysis Techniques," *Journal of Spacecraft and Rockets*, Vol. 19, July-Aug. 1982, pp. 326-337.

¹²Martin, J. A., "Ramjet Propulsion for Single-Stage-to-Orbit Vehicles," *Journal of Spacecraft and Rockets*, Vol. 15, Sept.-Oct. 1978, pp. 259-260.

¹³Wilhite, A. W., "Advanced Rocket Propulsion Technology Assessment for Future Space Transportation," *Journal of Spacecraft and Rockets*, Vol. 19, July-Aug. 1982, pp. 314-319.

¹⁴Wilhite, A. W., "Optimization of Rocket Propulsion System for Advanced Earth-to-Orbit Shuttles," *Journal of Spacecraft and Rockets*, Vol. 17, March-April 1980, pp. 99-104.

¹⁵Thelander, J. A., "Aerospacecraft Performance Optimization Considering Combination Airbreathing-Rocket Propulsive Systems," AIAA Paper 65-18, Jan. 1985.

¹⁶Venugopal, N., Grandhi, R. V., Hankey, W. L., and Belcher, P. J., "Combined Energy Management and Calculus of Variations Approach for Optimizing Hypersonic Vehicle Trajectories," *Journal of Computing Systems in Engineering*, Vol. 1, No. 2-4, 1990, pp. 591-600.

¹⁷Leingang, J. L., Donaldson, W. A., Watson, K. A., and Carrerio, L. R., "ETO—A Trajectory Program for Aerospace Vehicles," WRDC-TR-89-2023, Wright Patterson Air-Force Base, Ohio, June 1989.

James A. Martin
Associate Editor

Recommended Reading from the AIAA Progress in Astronautics and Aeronautics Series . . .



Thermal Design of Aeroassisted Orbital Transfer Vehicles

H. F. Nelson, editor

Underscoring the importance of sound thermophysical knowledge in spacecraft design, this volume emphasizes effective use of numerical analysis and presents recent advances and current thinking about the design of aeroassisted orbital transfer vehicles (AOTVs). Its 22 chapters cover flow field analysis, trajectories (including impact of atmospheric uncertainties and viscous interaction effects), thermal protection, and surface effects such as temperature-dependent reaction rate expressions for oxygen recombination; surface-slip equations for low-Reynolds-number multicomponent air flow, rate chemistry in flight regimes, and noncatalytic surfaces for metallic heat shields.

TO ORDER: Write, Phone or FAX:

American Institute of Aeronautics and Astronautics,
c/o TASC0, 9 Jay Gould Ct., P.O. Box 753, Waldorf, MD 20604
Phone (301) 645-5643, Dept. 415 ■ FAX (301) 843-0159

Sales Tax: CA residents, 7%; DC, 6%. For shipping and handling add \$4.75 for 1-4 books (call for rates for higher quantities). Orders under \$50.00 must be prepaid. Foreign orders must be prepaid. Please allow 4 weeks for delivery. Prices are subject to change without notice. Returns will be accepted within 15 days.

1985 566 pp., illus. Hardback
ISBN 0-915928-94-9
AIAA Members \$54.95
Nonmembers \$81.95
Order Number V-96